Am J Transl Res 2022;14(1):518-533
www.ajtr.org /ISSN:1943-8141/AJTR0137935

Original Article

circ_014260/miR-384/THBS1 aggravates spinal cord injury in rats by promoting neuronal apoptosis and endoplasmic reticulum stress

Yu Yao[1], Xin Zhang[1], Jun Xu[1], Feng Gao[1], Yanni Wu[2], Xintao Cui[1], Li Wei[1], Jie Jiang[3], Xintao Wang[1]

Departments of [1]Orthopedics, [2]Nephrology, The Second Affiliated Hospital of Harbin Medical University, Harbin 150001, Heilongjiang Province, China; [3]Department of Orthopedics, Hailun Traditional Chinese Medicine Hospital, Suihua 152300, Heilongjiang Province, China

Received August 2, 2021; Accepted December 3, 2021; Epub January 15, 2022; Published January 30, 2022

Abstract: Objective: To explore the mechanism of circ_014260 regulating neuronal apoptosis, oxidative stress, and endoplasmic reticulum stress in rats with spinal cord injury (SCI) *via* miR-384/THBS1 axis. Methods: T9-L10 spinal cord segments of Sprague Dawley rats were subjected to compression or contusion injuries after T10 laminectomy to establish rat models of SCI, which were then divided into SCI group, si-circ group and oe-circ group according to the transfection. There was another sham operation group which received no treatment. There were 10 rats in each group. The Basso-Beattie-Bresnahan scale and HE staining were used to evaluate the changes in neuronal motor function in rats with SCI. TUNEL staining was used to determine the neuronal apoptosis. Flow cytometry was used to measure the changes in H_2O_2-induced apoptosis of primary neurons. The activities of myeloperoxidase, malondialdehyde, superoxide dismutase and catalase were measured to evaluate the level of oxidative stress. Western blot was used to measure the expressions of CHOP and CRP78 (which are related to endoplasmic reticulum stress). Expression of circ_014260, miR-384 and THBS1 in tissues and cells was measured by qRT-PCR. RNase R restriction enzyme digestion and chromatin fractionation were used to identify the nature of circ_014260. Dual-luciferase reporter assay and RNA immunoprecipitation were used to verify the targeted binding relationship between circ_014260 and miR-384, as well as between miR-384 and THBS1. Results: Compared with the sham operation group or the untreated rat primary neurons (control group), increased expression of circ_014260 and THBS1 as well as decreased expression of miR-384 were observed in the spinal cord tissue from rats with SCI and in H_2O_2-treated primary neurons (all $P<0.05$). The results of both *in vivo* and *in vitro* experiments showed that knocking down circ_014260 could reduce neuronal apoptosis and inhibit oxidative stress and endoplasmic reticulum stress in rats with SCI (all $P<0.05$). Circ_014260 targetedly inhibited miR-384 to up-regulate the expression of THBS1. Both miR-384 inhibitor and THBS1 overexpression vector partially reversed the alleviated neuronal damage by knocking down circ_014260 (both $P<0.05$). Conclusion: Circ_014260 promotes neuronal damage in rats with SCI by inhibiting miR-384 to up-regulate the expression of THBS1. Thus, circ_014260 could possibly be a new molecular target of SCI.

Keywords: circ_014260, miR-384, THBS1, spinal cord injury

Introduction

Spinal cord injury (SCI), as a common injury of the sport system, mainly damages the central nervous system of the patients and may lead to paralysis of the limbs in severe cases [1]. Due to the complexity of the pathology and biological mechanism, there is still a lack of systematic understanding of the apoptosis mechanism of nerve cells after SCI, so further exploration is needed [2].

Non-coding RNAs (ncRNAs), as a type of genetic, epigenetic, and translational regulatory factors, are widely involved in physiological and pathological regulation processes [3]. Studies have found that ncRNAs, especially microRNAs (miRNAs) and circRNAs, participate in the progression of neurological diseases [4]. CircRNAs are a new type of endogenous ncRNAs, characterized by covalently closed loop structures with neither 5' caps nor 3'poly-A. CircRNAs are abundantly present in mammalian cells, more stable

than linear RNAs and more abundant in nervous system tissues than in other tissues [5]. Although the physiological functions of circRNAs in the nervous system have not been fully understood, one of the most widely studied functions of circRNAs is their role as miRNA sponges. For example, circPlek regulates the miR-135b/TGF-βR1 axis to promote the activation of fibroblasts in SCI [6]. Comprehensive analysis of circRNAs in the spinal cord can help to determine candidate diagnostic markers and therapeutic targets for SCI. Studies have shown that the expression of circ_014260 (chr1:155726970-155753880, NM_0010375-33) is up-regulated in traumatic SCI, but the regulatory effect and mechanism of circ_014-260 in SCI have not been reported [7]. As one of the key factors of post-transcriptional regulation of genes, miRNAs play an important role in the progress of SCI [8]. It is reported that miR-384-5p promotes the recovery of SCI in rats by inhibiting autophagy and endoplasmic reticulum stress (ERs) [9]. However, the possible regulatory mechanism of miR-384-5p in SCI remains to be further discussed, such as whether it interacts with other regulatory factors and participate in the progress of SCI. Thrombospondin 1 (TSP-1, THBS1) is an important extracellular matrix protein secreted by astrocytes. THBS1 increases rapidly in the injured spinal cord segment in rats. Decreasing the expression of THBS1 can effectively prevent pathological changes after SCI [10]. But the mechanism of THBS1 in SCI still needs to be further explored.

In this study, the circ_014260/miR-384/THBS1 interaction network was established to explore the relationship among circ_014260, miR-384 and THBS1, and their effect on neuronal damage in rats with SCI, so as to provide theoretical support for the diagnosis and treatment of SCI.

Materials and methods

Bioinformatics analysis

The SCI-related data set GSE114426 was obtained from the NCBI database (https://www.ncbi.nlm.nih.gov) to analyze the differentially expressed circRNAs in SCI. The analysis was performed in 3 rats with SCI and 3 rats in sham operation group. The differential filter criteria were adj. *P* value <0.05 and |LogFoldChange|>1. StarBase (http://starbase.sysu.edu.cn/index.php) and TSCD (http://gb.whu.edu.cn/TSCD/) were used to obtain the downstream target miRNAs of circ_014260. TargetScan (http://www.targetscan.org/vert_72/), miRDB (http://mirdb.org) and online prediction website StarBase were used to predict the downstream target genes of miR-384. DAVID (http://david.ncifcrf.gov) was used for Gene Ontology (GO) enrichment analysis.

Grouping and model establishment

Forty male SD rats (8-10 weeks old, purchased from Beijing Huafukang Biotechnology Co., Ltd., China) were randomly divided into sham operation group, SCI group, si-circ group and oe-circ group, each with 10 rats. Rats in the SCI group, si-circ group and oe-circ group were established as model of SCI. The animals were intraperitoneally injected with 3% pentobarbital sodium (157175, 30 mg/kg, Hubei Hongyunlong Biotechnology Co., Ltd., China) for anesthesia. The spinous process and lamina of the rat segment T9-L10 were selected as injury area and subjected to compression or contusion injuries with a hitting device. Rat showing spastic swinging at tail, hind limbs and body immediately was considered successfully modeled. Rats in the sham operation group were treated with T10 laminectomy without giving compression or contusion injuries. After 24 hours, rats in the si-circ group and oe-circ group were intrathecally injected with lentiviral vectors (2 μg pLO5-ciR, Guangzhou Geneseed Biotech Co., Ltd, China) containing si-circ (circ_014260 small interfering RNA) or oe-circ (circ_014260 overexpression vector) into the spinal cord. The lentivirus was injected from L5-6 interspinous space with a microsyringe (vertically and slowly inserted) after the tail of rat flailed and cerebrospinal fluid could be seen by withdrawing. The knock-down or over-expression efficiency of circ_014260 in the rat spinal cord tissue was measured by qRT-PCR. All animal experiment procedures were completed in strict accordance with the guidelines for the care and use of experimental animals. This study was approved by the animal ethics committee of our hospital.

Culture of spinal cord neurons

According to the operations in previous report, 4-day-old newborn SD rats (purchased from Beijing Huafukang Biotechnology Co., Ltd.,

Table 1. Transfection sequence

Gene	from 5' to 3'
si-circ	AACAAGGTGGCCCTGTGGAGA
si-NC	AACAAGGTGGCCCTGTGGAGA
miR-384 inhibitor	CAACAAAAUCACUGAUGCUGGA
miR-NC	UUUGUACUACACAAAAGUACUG

China) were anesthetized with 2% sodium pentobarbital at a concentration of 40 mg/kg, sacrificed by using CO_2, immersed in 75% ethanol for 15 min and rinsed using Hank's balanced salt solution (Shanghai Yuchun Biotechnology Co., Ltd., China) [9]. The spinal cord was separated under aseptic conditions and the surface fibrous vascular membrane was stripped in pre-cooled Hank's balanced salt solution. The spinal cord was then cut into particles of 1 mm^3, digested in 0.25% trypsin (SH30042, Shanghai Lianshuo Biotechnology Co., Ltd., China) for 20 min and centrifuged at 1000 r/min for 5 min (centrifugal radius: 13.5 cm). After the supernatant was discarded, the samples were resuspended in Dulbecco's modified Eagle's medium (Shanghai Yuchun Biotechnology Co., Ltd., China) containing 20% fetal bovine serum, inoculated in a 6-well plate at a density of 5×10^5 cells/mL. To increase the purity of the neurons, the samples were added with cytarabine (final concentration: 3 mol/L) and cultured for 3 days. DAPI staining was used to obtain the total number of cells. The β-III Tubulin positive cells stained by fluorescein isothiocyanate (FITC) were neurons. The number of positive cells was counted by Image J software. The positive rate of cells = number of positive cells/total number of cells ×100%.

The neurons were exposed to 100 μmol/L H_2O_2 solution (12 h). Circ_014260 and THBS1 were overexpressed, and their gene full length sequences were cloned into pcDNA3.1 plasmid and named oe-circ/pcDNA3.1-ThBS1. Blank plasmid (pcDNA3.1-NC/oe-NC) was used as control. The neurons were transfected with single si-circ (si-NC), oe-circ (oe-NC), miR-384 inhibitor or its control (miR-NC), pcDNA3.1-THBS1 or pcDNA3.1-NC, or in combination with Lipofectamine3000 (L3000015, Beijing Zhijie Fangyuan Technology Co., Ltd., China). The above plasmids or vectors were all purchased from Jiman Biotechnology Co., Ltd., China. Follow-up determination of neuronal cells was performed 48 h after transfection. The transfection sequences used in this experiment are shown in **Table 1**.

HE staining

After 7 days postoperative behavioral observation, rats in each group were sacrificed by using CO_2. First, the tissue was directly separated at the original incision on the back to expose the spinal cord. Spinal cord tissues (2 cm around the lesion) were taken and fixed with 4% paraformaldehyde (P0099, Shanghai Beyotime Biotechnology Co., Ltd., China) for 24 h. After embedding with paraffin, slices of 5 μm in thickness were obtained. Second, the slices were treated with 75% xylene for 15 and 5 min, respectively, washed with 50% xylene, 50% ethanol, and then with 100%, 95%, 85%, 70%, 50% ethanol and water in turn. Third, the slices were stained in hematoxylin for about 20 min and rinsed with tap water for 15 min to make them blue. Thereafter, the slices were discolored in 1% hydrochloric acid ethanol solution, and then rinsed with water. Fourth, the slices were placed in 50%, 70%, and 80% ethanol for 5 min, respectively, then stained with 0.5% eosin ethanol solution for 3 min, washed in 95% ethanol and placed in absolute ethanol for 5 min. Lastly, the slides were sealed with neutral gum, observed, and photographed under a microscope.

Evaluation of motor function

Seven days after modeling, Basso, Beattie & Bresnahan locomotor rating (BBB) scale was used to evaluate the motor function impairment of the hind limbs of rats with SCI [9]. Joint activity of hind limb was assessed in early phase (0-7 points). Gait and coordination function of the hind limb was assessed during middle and late stage (8-13 points). Fine motor skills of paws were assessed in the final stage (14-21 points). Completely normal motor function of the hind limbs was seen as 21 points. The BBB score of each group of rats was calculated to evaluate the changes of motor function.

Flow cytometry

The AnnexinV-FITC/PI apoptosis double staining kit (556547, Beijing Livining Biotechnology Co., Ltd., China) was used to measure changes of neuronal apoptosis. Neuronal cells were centrifuged for 5 min at 2000 r/min, washed twice with 1 mL of 10 mM phosphate-buffered saline (PBS) and suspended in 400 μL 1× binding buffer. The cell suspension was added with 5 μL of AnnexinV-FITC and incubated for 15 min at 4°C

Table 2. qRT-PCR premier sequence

Name	Sequence (5'-3')
circ_014260	
Forward	ATCGCTGCTAGCTACTTAGCTA
Reverse	CTGATCGTGAACTGCCGTGGCTA
miR-384	
Forward	TGTTAAATCAGGAATTTTAA
Reverse	TGTTACAGGCATTATGAA
THBS1	
Forward	GCTCCAGTCCTACCAGTGTC
Reverse	TCAGTCACTTGCGGATGCT
GAPDH	
Forward	ACCACAGTC CATGCCATCAC
Reverse	TCCACCACCCT GTT GCTGTA
U6	
Forward	GCUUCGGCAGCACAUAUACUAAA
Reverse	CGCUUCACGAAUUUGCGUGUCAU

in dark, then added with 10 μL of PI and reacted for 15 min in dark. A flow cytometer (RZ, Shanghai Ranzhe Equipment Co., Ltd., China) was then used to detect cell apoptosis.

TUNEL staining

TUNEL assay kits (40306ES60, Yisheng Biotechnology Co., Ltd., Shanghai, China) were used to detect changes in spinal cord neuronal apoptosis. The slices were immersed in xylene at room temperature for 5 min (repeat once) and in 100% ethanol for 5 min (repeat once), washed in 90%, 80%, and 70% ethanol, respectively, 3 min each time, and rinsed with PBS. Each sample was added with 100 μL of Proteinase K solution (20 μg/mL), incubated at room temperature for 20 min, rinsed with PBS twice, then added with 100 μL 1× equilibration buffer dropwise and incubated at room temperature for 30 min. After discard of the 1× equilibration buffer, the cells were added with 50 μL TdT incubation buffer in a 5 cm^2 area and incubated at 37°C for 60 min in dark. After incubating in PBS for 5 min, the cells were washed with PBS twice, and stained with propidium iodide solution (1 μg/mL) for 5 min in dark. The samples were washed with deionized water, stood for 5 min (repeat twice), and then analyzed under a fluorescence microscope.

Western blot

The collected spinal cord samples were washed with PBS, added with RIPA lysis buffer (JLC-SJ2497, Jingkang Bioengineering Co., Ltd., Shanghai, China), extracted for total protein and measured for protein concentration using BCA protein quantification kits (JLC-SJ2508, Jingkang Bioengineering Co., Ltd., Shanghai, China). Thereafter, 20 μg of protein was electrophoretically transferred through 10% SDS-PAGE. The separated protein was transferred to a PVDF membrane, blocked with 5% skimmed milk, and incubated with primary antibodies against THBS1 (1:1000, ab226950, Abcam, UK), CHOP (1:1000, ab233121, Abcam, UK), GRP78 (1:1000, ab108615, Abcam, UK) and GAPDH (1:1000, ab8245, Abcam, UK) overnight at 4°C. The samples were then washed with TBST buffer, incubated with HRP-labeled goat anti-rabbit IgG (1:2000, F030212, Beijing Biolab Technology Co., Ltd., China) at room temperature for 1 h, and washed with TBST buffer repeatedly. Then, ECL chemiluminescence kits (36222ES76, Yisheng Biotechnology Co., Ltd., Shanghai, China) were used to visualize the protein bands.

Determination of oxidative stress parameters

According to the instructions, corresponding kits were used to determine the concentration or activity of myeloperoxidase (MPO, colorimetric method, A044-1-1), malondialdehyde (MDA, TBA method, A003-1-2), superoxide dismutase (SOD, WST-1 method, A001-3-2) and catalase (CAT, ammonium molybdate method, A007-1-1) in the supernatant of neuronal cells after transfection. All the kits were from Nanjing Jiancheng Institute of Bioengineering, China.

qRT-PCR

Trizol reagent (R21086, Shanghai Yuanye Biotechnology Co., Ltd., China) was used to extract total RNA from SCI tissue or neuronal cells. Reverse transcription kit (A0010, Shanghai Haifang Biotechnology Co., Ltd., China) was used to synthesize cDNA. The PCR reaction system (20 μL) included 10× Buffer (2 μL), cNTP (1.6 μL), TaQ-enzyme (1 μL), double distilled water (11.8 μL), cDNA (2 μL) and primer (1.6 μL). The reaction conditions were as follows: pre-denaturation at 95°C for 10 min, denaturation at 95°C for 15 s and annealing at 60°C for 30 s, with a total of 45 cycles. U6 was the internal reference for miR-384, and GAPDH was the internal reference for circ_014260 and THBS1. The $2^{-\Delta\Delta Ct}$ formula was used to calculate the relative gene expression. The primer sequences are shown in **Table 2**.

Dual-luciferase reporter assay

Circ_014260 or THBS1 3'UTR sequences containing wild-type or mutant miR-384 binding sites were constructed and subcloned into pGL3 luciferase reporter vector (Shanghai Haiji Hoge Biotechnology, China) to generate WT-circ_014260/WT-THBS1 and MUT-circ_014260/MUT-THBS1 reporter plasmid. The reporter plasmid and miR-384 mimic or its negative control (miR-NC) were co-transfected with HEK-293T cells (Cell Bank of Chinese Academy of Sciences, Shanghai, China). After 48 h of transfection, Dual luciferase reporter kit (D0010, Beijing Soleibao Technology Co., Ltd., China) was used to determine the luciferase activity. The ratio of firefly luciferase activity to renilla luciferase activity was considered to be the relative activity of luciferase.

RNA immunoprecipitation (RIP)

The RIP was performed using Magna RIP™ RNA-binding protein immunoprecipitation kit (17-700, Shanghai Chuangsai Technology Co., Ltd., China). Rat neuronal cells were lysed with RIP buffer and incubated with magnetic beads bound to negative control antibody IgG (5 μg, ab172730, Abcam, UK) or human AGO2 antibody (5 μg, ab32381, Abcam, UK) at 4°C overnight. The samples were then incubated with proteinase K for 30 min. The immunoprecipitated RNA was extracted with Trizol reagent, and the relative expressions of circ_014260 and miR-384 were measured by qRT-PCR.

RNase R restriction enzyme digestion

Trizol reagent was used to extract total RNA (2 μg) from rat neurons. The total RNA was added with RNase R (3 U/μg, R0301, Guangzhou Jisai Biotechnology Co., Ltd., China) and incubated at 37°C for 30 min. Then qRT-PCR was used to measure the levels of circ_014260 and GON4L, with GAPDH as internal reference. The $2^{-\Delta\Delta Ct}$ formula was used to calculate the relative expression of circ_014260 and GON4L.

Chromatin fractionation

Cytoplasmic and nuclear RNA purification kit (NGB-21000, Amictech Technology Co., Ltd., China) was used to isolate cytoplasmic and nuclear RNA from rat neurons. Then, qRT-PCR was used to determine the expression level of RNA molecules in the nucleus and cytoplasm. U6 was used as control for nucleus, and GAPDH was used as control for cytoplasm.

Statistical analyses

SPSS 22.0 software was used for data analyses. Measurement data were expressed in the form of mean ± standard deviation ($\bar{x}\pm sd$). Count data were represented by n and processed by chi-square test or Fisher's exact test. Measurement data conforming to the normal distribution were compared using t test between two groups and compared using one-way analysis of variance and Bonferroni correction among multiple groups. For measurement data that did not meet normal distribution, Mann-Whitney U test was performed for the comparison between two groups, and Bonferroni correction was used for the pairwise comparisons in multiple groups. A difference of $P<0.05$ was considered statistically significant.

Results

Results of bioinformatics analysis

The differentially expressed circRNAs in the GSE114426 data set were plotted as a volcano map (**Figure 1A**), and the top 5 circRNAs according to the differential expression multiple (log2FC) that were significantly and highly expressed in SCI were selected to plot a heat map (**Figure 1B**). Based on previous research, the possible role and mechanism of circ_014260 in SCI was selected to be discussed. Downstream target miRNAs of circ_014260 were obtained from StarBase and online prediction website TSCD, and the intersection included hsa-miR-330-3p, hsa-miR-432-5p, hsa-miR-1251-5p, hsa-miR-942- 5p, hsa-miR-384 and hsa-miR-3613-5p (**Figure 1C**). The binding sites of circ_014260 and miR-384 are shown in **Figure 1D**. It was previously confirmed that miR-384 was down-regulated and played a role in SCI, so miR-384 was chosen for subsequent analyses. Downstream target genes of miR-384 were obtained in StarBase, miRDB and TargetScan, and the intersection included 341 genes (**Figure 1E**). Subsequently, the GO term enrichment was performed on the online prediction website

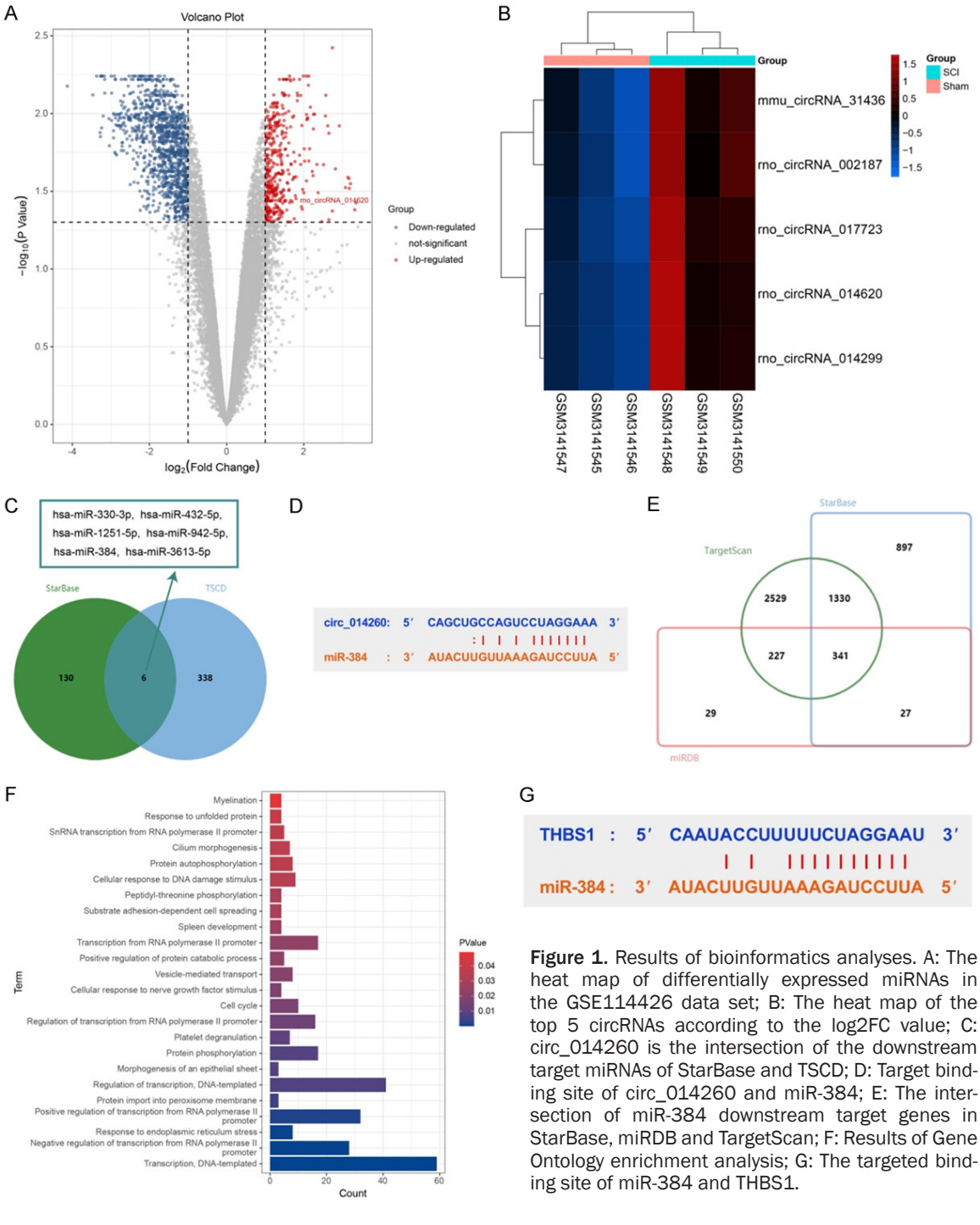

Figure 1. Results of bioinformatics analyses. A: The heat map of differentially expressed miRNAs in the GSE114426 data set; B: The heat map of the top 5 circRNAs according to the log2FC value; C: circ_014260 is the intersection of the downstream target miRNAs of StarBase and TSCD; D: Target binding site of circ_014260 and miR-384; E: The intersection of miR-384 downstream target genes in StarBase, miRDB and TargetScan; F: Results of Gene Ontology enrichment analysis; G: The targeted binding site of miR-384 and THBS1.

DAVID. The GO Terms with P<0.05 were plotted as **Figure 1F**. It was noted that 8 target genes were significantly enriched in the GO Term of ERs. Among them, only THBS1 (TSP-1) was reported to be related to SCI, so THBS1 was further studied. The binding sites of miR-384 and THBS1 are shown in **Figure 1G**.

circ_014260 and THBS1 were up-regulated and miR-384 was down-regulated in SCI

Image J software was used to count the neuronal cells, stained positive by tubulin. The isolated neurons accounted for about 81% of the total number of cells (**Figure 2**). Subsequently,

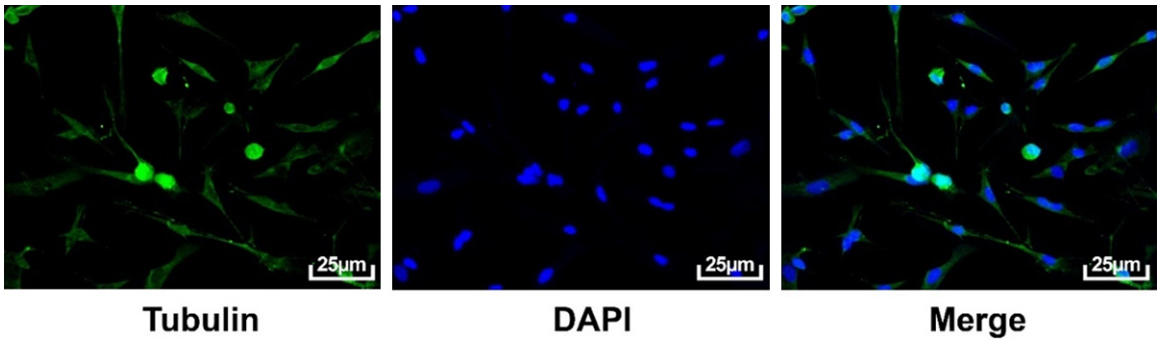

Figure 2. Identification of neurons by tubulin staining.

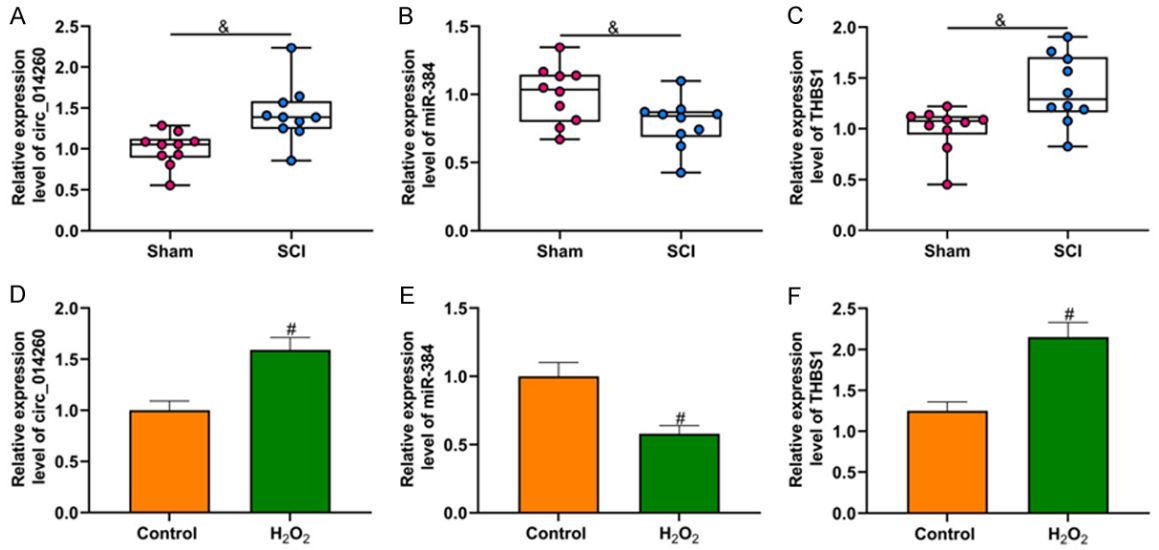

Figure 3. Circ_014260 and THBS1 were up-regulated and miR-384 was down-regulated in SCI. A: Expression of circ_014260 in sham operation group and SCI group measured by qRT-PCR (n=10); B: Expression of miR-384 in the sham operation group and SCI group measured by qRT-PCR (n=10); C: Expression of THBS1 in the sham operation group and SCI group measured by qRT-PCR (n=10); D: Expression of circ_014260 in untreated and H_2O_2-treated rat neurons measured by qRT-PCR (n=3); E: Expression of miR-384 in untreated and H_2O_2-treated rat neurons measured by qRT-PCR (n=3); F: Expression of THBS1 in untreated and H_2O_2-treated rat neurons measured by qRT-PCR (n=3). Compared with sham operation group, $^{\&}P<0.05$; compared with control group, $^{\#}P<0.05$. SCI: spinal cord injury.

the expressions of circ_014260, miR-384 and THBS1 in SCI were measured. Results of qRT-PCR showed that the expressions of circ_014260 and THBS1 in the spinal cord tissue of SCI rats were higher than those of the sham operation group, while results of miR-384 were the opposite (all P<0.05, **Figure 3A-C**). Compared with untreated rat neurons, the expression of circ_014260 and THBS1 increased, while the expression of miR-384 decreased in H_2O_2-induced rat neurons (all P<0.05, **Figure 3D-F**). The above results indicate that the abnormal expression of circ_014260, miR-384 and THBS1 in SCI may be related to disease progression.

circ_014260 induced neuronal cell apoptosis, oxidative stress, and ERs in SCI

The function of circ_014260 in SCI was subsequently explored. The circ_014260 knockdown vector (si-circ) or the overexpression vector (oe-circ) was used to interfere with the expression of circ_014260 in H_2O_2-induced rat neurons. Results of qRT-PCR showed that transfection of si-circ significantly reduced the expression of circ_014260 in neurons, and the transfection of oe-circ significantly increased the expression of circ_014260 (all P<0.05, **Figure 4A**). Analysis of data from Flow cytometry showed that knocking down circ_014260 sig-

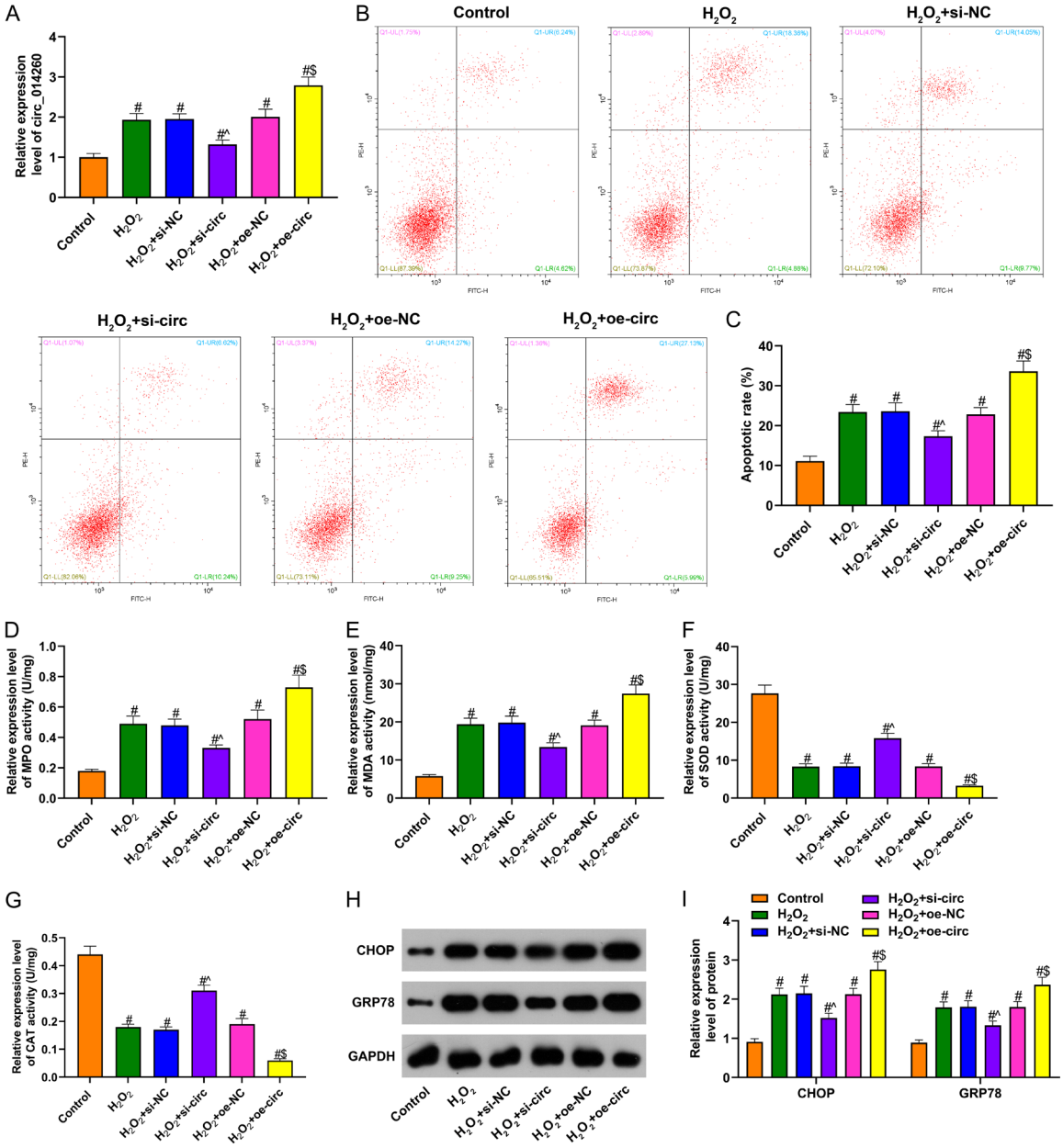

Figure 4. Circ_014260 induced neuronal cell apoptosis, oxidative stress and ERs in SCI. A: Transfection efficiency of si-circ or oe-circ measured by qRT-PCR (n=3); B, C: Changes in neuronal apoptosis detected by flow cytometry (n=3); D: Changes in MPO activity measured by Elisa (n=3); E: Changes in MDA activity measured by Elisa (n=3); F: Changes in SOD activity measured by Elisa (n=3); G: Changes in CAT activity measured by Elisa (n=3); H, I: Protein levels of CHOP and GRP78 measured by Western blot (n=3). Compared with control group, #P<0.05; compared with H_2O_2+si-NC group, ^P<0.05; compared with H_2O_2+oe-NC group, $P<0.05. ERs: endoplasmic reticulum stress, SCI: spinal cord injury, MPO: myeloperoxidase, MDA: malondialdehyde; SOD: superoxide dismutase; CAT: catalase.

nificantly reduced the apoptosis of neurons, while overexpression of circ_014260 resulted the opposite (both P<0.05, **Figure 4B**, **4C**). Results of Elisa showed that the activities of MPO and MDA increased, and the activities of SOD and CAT decreased in the supernatant of rat neurons treated by H_2O_2. The knockdown of circ_014260 inhibited these results, while the overexpression of circ_014260 did the opposite (all P<0.05, **Figure 4D-G**). Data from Western blot showed that compared with the control group, the protein levels of CHOP and

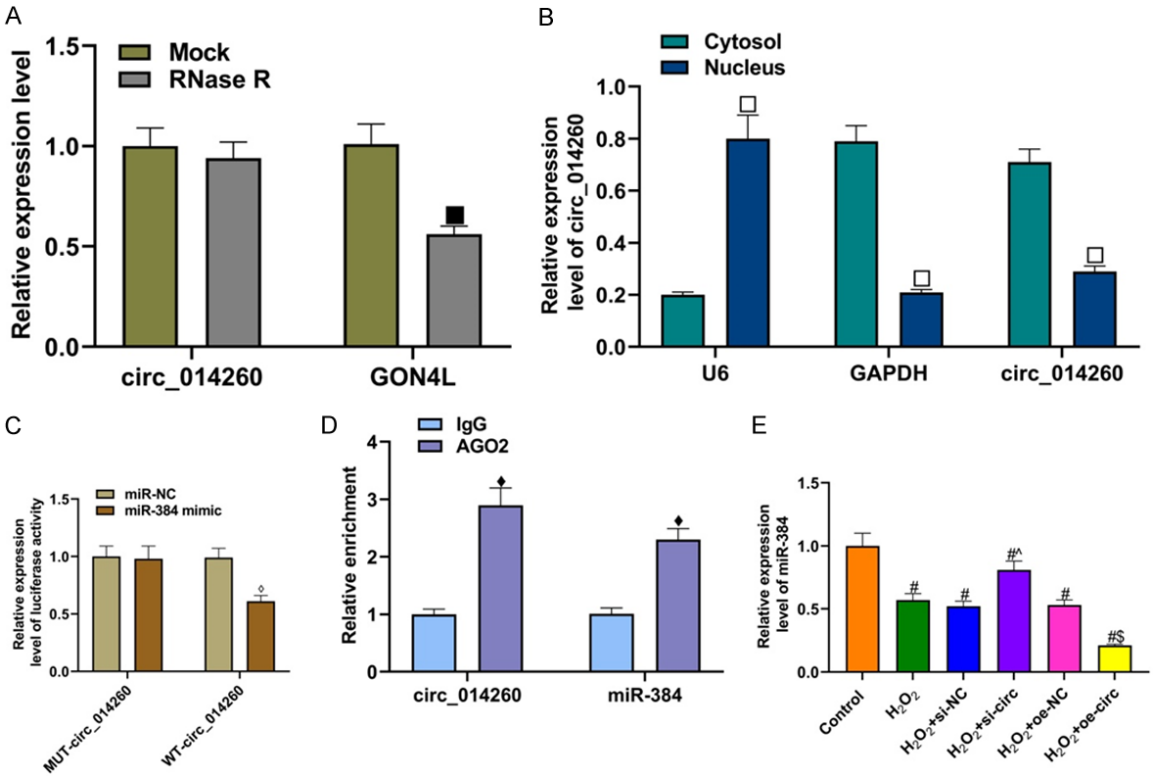

Figure 5. Circ_014260 was proved to be a competitive endogenous RNA for miR-384. A: Results of RNase restriction enzyme digestion (n=3); B: Results of chromatin fractionation (n=3); C: Results of Dual-luciferase reporter assay (n=3); D: Results of RNA immunoprecipitation (n=3); E: Level of miR-384 in rat neurons measured by qRT-PCR (n=3). Compared with the Mock group, ▪P<0.05; compared with the Cytosol group, □P<0.05; compared with miR-NC group, ◇P<0.05; compared with the IgG group, ♦P<0.05; compared with control group, #P<0.05; compared with H_2O_2+si-NC group, ^P<0.05; compared with H_2O_2+oe-NC group, $P<0.05.

GRP78 were decreased in the si-circ group while increased in the oe-circ group (all P<0.05, **Figure 4H**, **4I**). The above results indicate that circ_014260 can aggravate H_2O_2-induced neuronal apoptosis, oxidative stress and ERs in rats.

circ_014260 was approved to be a competitive endogenous RNA for miR-384

The results of RNase digestion confirmed that circ_014260 had a stable ring structure (P<0.05, **Figure 5A**). Data from chromatin fractionation showed that circ_014260 was mainly located in the cytoplasm and could stably exert function of competitive endogenous RNA (P<0.05, **Figure 5B**). In order to verify the relationship between circ_014260 and miR-384, Dual-luciferase reporter assay and RIP were carried out. The results showed that compared with the miR-NC group, miR-384 mimic significantly inhibited the fluorescence activity of WT-circ_014260 but had almost no effect on the fluorescence activity of MUT-circ_014260 (P<0.05, **Figure 5C**). The RIP showed that compared with the IgG group, circ_014260 and miR-384 were significantly enriched in the AGO2 antibody precipitation (P<0.05, **Figure 5D**). In addition, results of qRT-PCR found that knocking down circ_014260 in H_2O_2-treated rat neurons increased the expression of miR-384, while overexpression of circ_014260 decreased the expression of miR-384 (all P<0.05, **Figure 5E**). The above results indicate that circ_014260, as a competitive endogenous RNA of miR-384, can negatively regulate its expression.

Inhibition of miR-384 partly rescued the neuronal damage from knockdown of circ_014260

To subsequently discuss the mechanism of circ_014260 and miR-384 in SCI, si-circ and miR-384 inhibitor were co-transfected into

H_2O_2-induced rat neurons. As compared with the control group, the expression of miR-384 was decreased in H_2O_2-treated neurons. Knockdown of si-circ_014260 promoted the expression of miR-384, but this effect was partially rescued by mirR-384 inhibitor (P<0.05, **Figure 6A**). Functional test showed that neuronal apoptosis was reduced by knocking down circ_014260 but increased by miR-384 inhibition (P<0.05, **Figure 6B**, **6C**). Compared with the H_2O_2+si-circ+miR-NC group, H_2O_2+si-circ+miR-384 inhibitor significantly reduced the concentrations of SOD and CAT but increased the concentrations of MPO and MDA (all P<0.05, **Figure 6D-G**). In addition, the protein expressions of CHOP and GRP78 were increased in the H_2O_2+si-circ+miR-384 inhibitor group as compared with the H_2O_2+si-circ+miR-NC group (both P<0.05, **Figure 6H**, **6I**). The above results indicate that inhibition of miR-384 can partially reverse the improvement in neuronal damage by the knockdown of circ_014260.

THBS1 was proved to be the target gene of miR-384

Results of Dual-luciferase reporter assay showed that compared with the miR-NC group, miR-384 mimic significantly inhibited the fluorescence activity of WT-THBS1, but had almost no effect on the fluorescence activity of MUT-THBS1 (P<0.05, **Figure 7A**). Data from RIP showed that compared with the IgG group, the AGO2 antibody precipitation was enriched in higher levels of THBS1 and miR-384 (P<0.05, **Figure 7B**). Results of qRT-PCR showed that in H_2O_2-treated rat neurons, knocking down circ_014260 inhibited the expression of THBS1 (P<0.05, **Figure 7C**). Overexpression of circ_014260 up-regulated the expression of THBS1. In addition, inhibition of miR-384 partially rescued the expression of THBS1 that was down-regulated by knockdown of circ_014260 (P<0.05, **Figure 7D**). These results indicate that THBS1, as a target gene of miR-384, is inhibited by miR-384 and promoted by circ_014260.

Overexpression of THBS1 partially reversed the neuronal damage reduced by knocking down circ_014260

The THBS1 overexpression vector (pcDNA3.1-THBS1) and si-circ were co-transfected into H_2O_2-treated rat neurons for functional exploration. The transfection of pcDNA3.1-THBS1 significantly increased THBS1 level that was inhibited by knocking down circ_014260 (P<0.05, **Figure 8A**). Neuronal apoptosis was decreased by down-regulation of circ_014260 but increased after THBS1 was up-regulated (P<0.05, **Figures 8B**, **7C**). Compared with H_2O_2+si-circ+pcDNA3.1-NC, pcDNA3.1-THBS1 significantly reduced the concentrations of SOD and CAT, but increased the concentrations of MPO and MDA (all P<0.05, **Figure 8D-G**). Additionally, overexpression of THBS1 also increased the protein expressions of CHOP and GRP78 which were reduced by si-circ (both P<0.05, **Figure 8H**, **8I**). The above results indicate that circ_014260 can aggravate neuronal damage in SCI rats by up-regulating THBS1.

Knockdown of circ_014260 reduced neuronal damage in rats with SCI

In vivo experiments were conducted to explore the effect of circ_014260 in rats with SCI. The lentiviral vector of si-circ or oe-circ was intrathecally injected into the spinal cord of rats to interfere with the expression of circ_014260. It was shown that si-circ significantly reduced while oe-circ increased the expression of circ_014260 (both P<0.05, **Figure 9A**). As compared with the SCI group, the si-circ group showed decreased spinal cord tissue fragmentation, decreased spinal cavity area, decreased number of neurons apoptosis and increased BBB score (all P<0.05, **Figure 9B-F**). Overexpression of circ_014260 aggravated spinal cord tissue fragmentation in SCI rats, increased spinal cavity area and number of neuronal apoptosis, and decreased BBB score (all P<0.05, **Figure 9B-E**). These results indicate that down-regulating the expression of circ_014260 can help alleviate neuronal damage in rats with SCI.

Discussion

The pathological mechanism of SCI has not been fully elucidated, so the clinical treatment and related scientific research are still full of challenges. Therefore, exploration of new molecular biomarkers needs to be addressed. Study has shown that reducing neuronal cell damage is beneficial to restore the motor func-

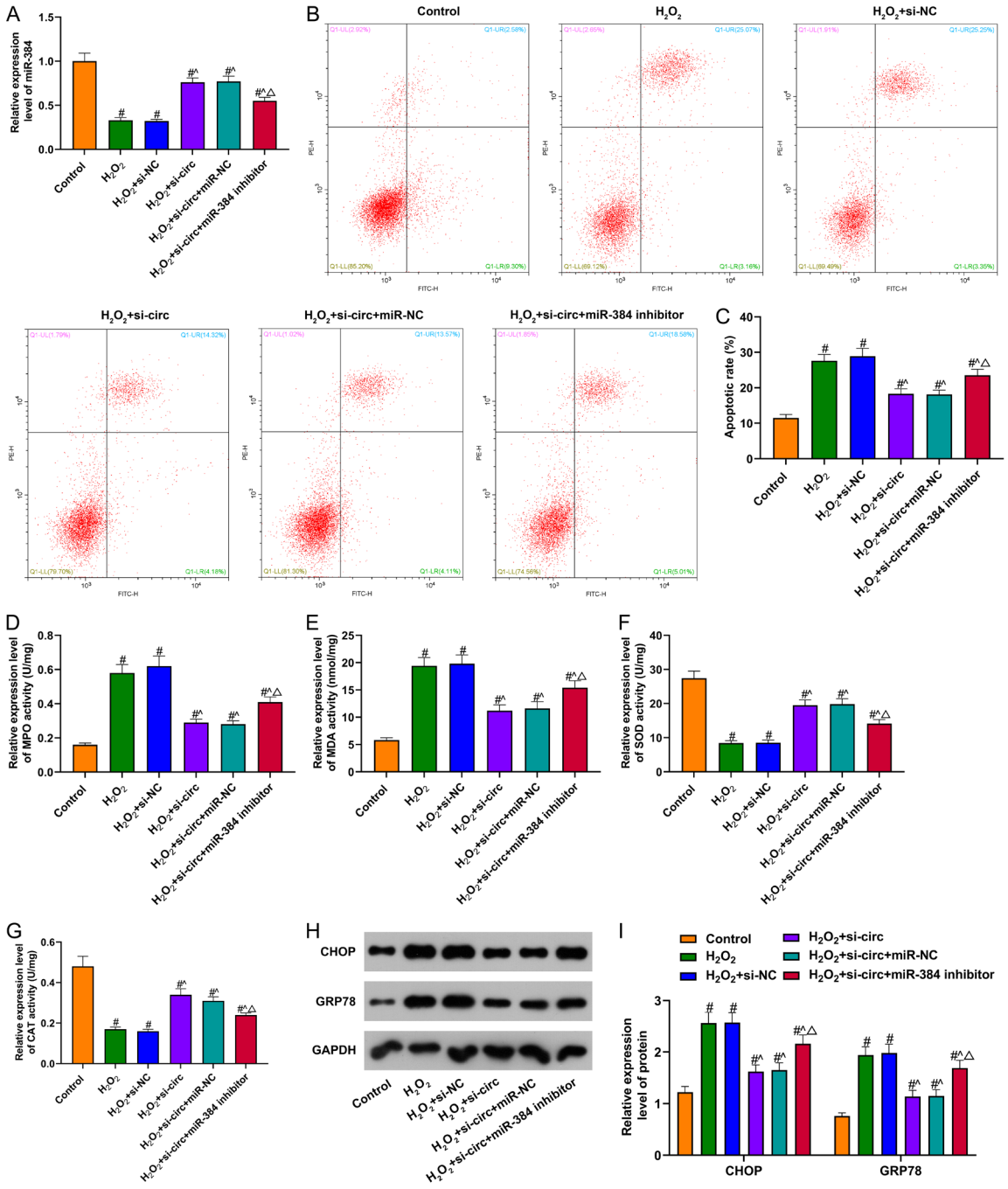

Figure 6. Inhibition of miR-384 aggravated the neuronal damage alleviated by downregulation of circ_014260. A: Level of miR-384 measured by qRT-PCR (n=3); B, C: Changes in neuronal apoptosis detected by flow cytometry (n=3); D: Changes in MPO activity measured by Elisa (n=3); E: Changes in MDA activity measured by Elisa (n=3); F: Changes in SOD activity measured by Elisa (n=3); G: Changes in CAT activity measured by Elisa (n=3); H, I: Protein levels of CHOP and GRP78 measured by Western blot (n=3). Compared with control group, #P<0.05; compared with H_2O_2+si-NC group, ^P<0.05; compared with H_2O_2+si-circ+miR-NC group, △P<0.05. MPO: myeloperoxidase; MDA: malondialdehyde; SOD: superoxide dismutase; CAT: catalase.

tion after SCI [11]. The results of this study showed that the expression of circ_014260 increased in both the rat model of SCI and the H_2O_2-treated neuronal cells. Knockdown of

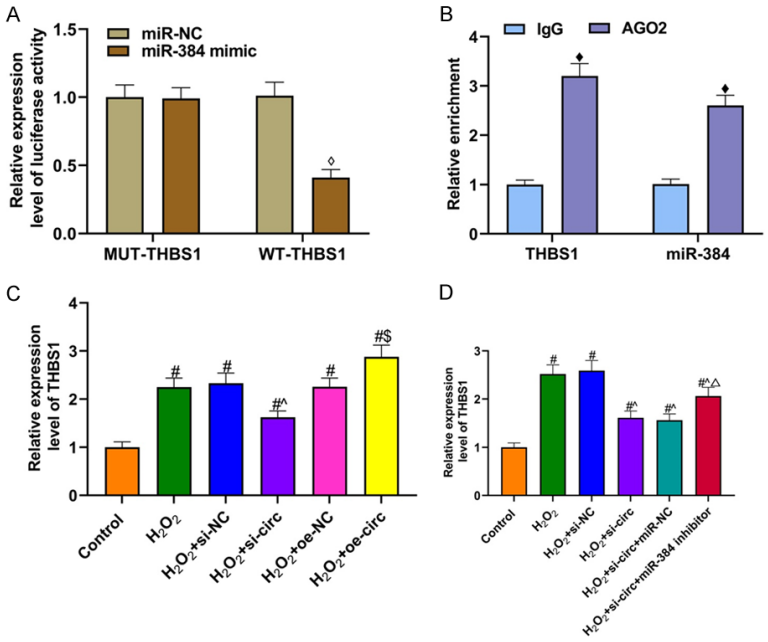

Figure 7. THBS1 was the target gene of miR-384. A: Results of Dual-luciferase reporter assay (n=3); B: Results of RNA immunoprecipitation (n=3); C, D: Level of THBS1 measured by qRT-PCR (n=3). Compared with miR-NC group, ◊P<0.05; compared with the IgG group, ♦P<0.05; Compared with control group, #P<0.05; compared with H_2O_2+si-NC group, ^P<0.05; compared with H_2O_2+si-circ+miR-NC group, △P<0.05.

circ_014260 can help alleviate neuronal damage in rats with SCI and effectively restore motor function. Additionally, as a competitive endogenous RNA, circ_014260 can up-regulate the expression of THBS1 by adsorbing miR-384 to promote neuronal apoptosis, oxidative stress and ERs, thereby aggravating SCI.

Previous studies have found that circRNAs have tissue-specific and cell-specific expression patterns [12, 13]. The expression levels of most circRNAs are lower than their linear transcripts [14]. However, in some cases, especially circRNAs in the central nervous system may have much higher expression than the corresponding linear transcripts [15]. For example, circRNAs are highly expressed in the process of neurodevelopment, degeneration, transmitter release, and axon growth [16]. In this study, the differentially expressed circRNA after SCI was analyzed, and we found circ_014260. Previous studies showed that circ_014260 was significantly up-regulated after SCI, which is consistent with the data of our study [7]. It is reported that secondary oxidative stress response after SCI is significantly related to the prognosis of patients, and the main oxidative stress molecules include pro-oxidant substances (MPO and MDA, etc.) and antioxidant substances (SOD and CAT, etc.) [17, 18]. This study found that down-regulating the expression of circ_014260 effectively inhibited the activity of MPO and MDA and increased the concentrations of SOD and CAT in H_2O_2-treated neuronal cells, while overexpression of circ_014260 reversed these effects. It is suggested that circ_014260 can promote the oxidative stress response of neurons after SCI, thereby aggravating oxidative damage. ER stress (ERs) is one of the apoptosis pathways discovered in recent years. High levels of CHOP and GRP78 can induce neuronal cell apoptosis [19, 20]. In this study, Western blot was used to measure the protein levels of CHOP and GRP78. The data showed that knocking down circ_014260 significantly inhibited while overexpression of circ_014260 promoted the expressions of CHOP and GRP78. It is suggested that circ_014260 can increase neuronal cell apoptosis by promoting ERs. The experimental data of flow cytometry further confirmed the pro-apoptotic effect of circ_014260 on neurons after SCI. In addition, in vitro experiments showed that inhibiting circ_014260 significantly reduced neuronal apoptosis and necrosis in the spinal cord tissue, and effectively restored motor function in rats with SCI, while overexpression of circ_014260 significantly aggravated SCI. The above results suggest that circ_014260 can aggravate neuronal damage in rats with SCI by promoting neuronal cell apoptosis, oxidative stress and ERs, and circ_014260 is possibly an effective target for the treatment of SCI.

In order to further determine the mechanism of circ_014260 in the pathological process of SCI, this study used StarBase and TSCD for screening and found that circ_014260 could specifically bind to miR-384. Previous studies

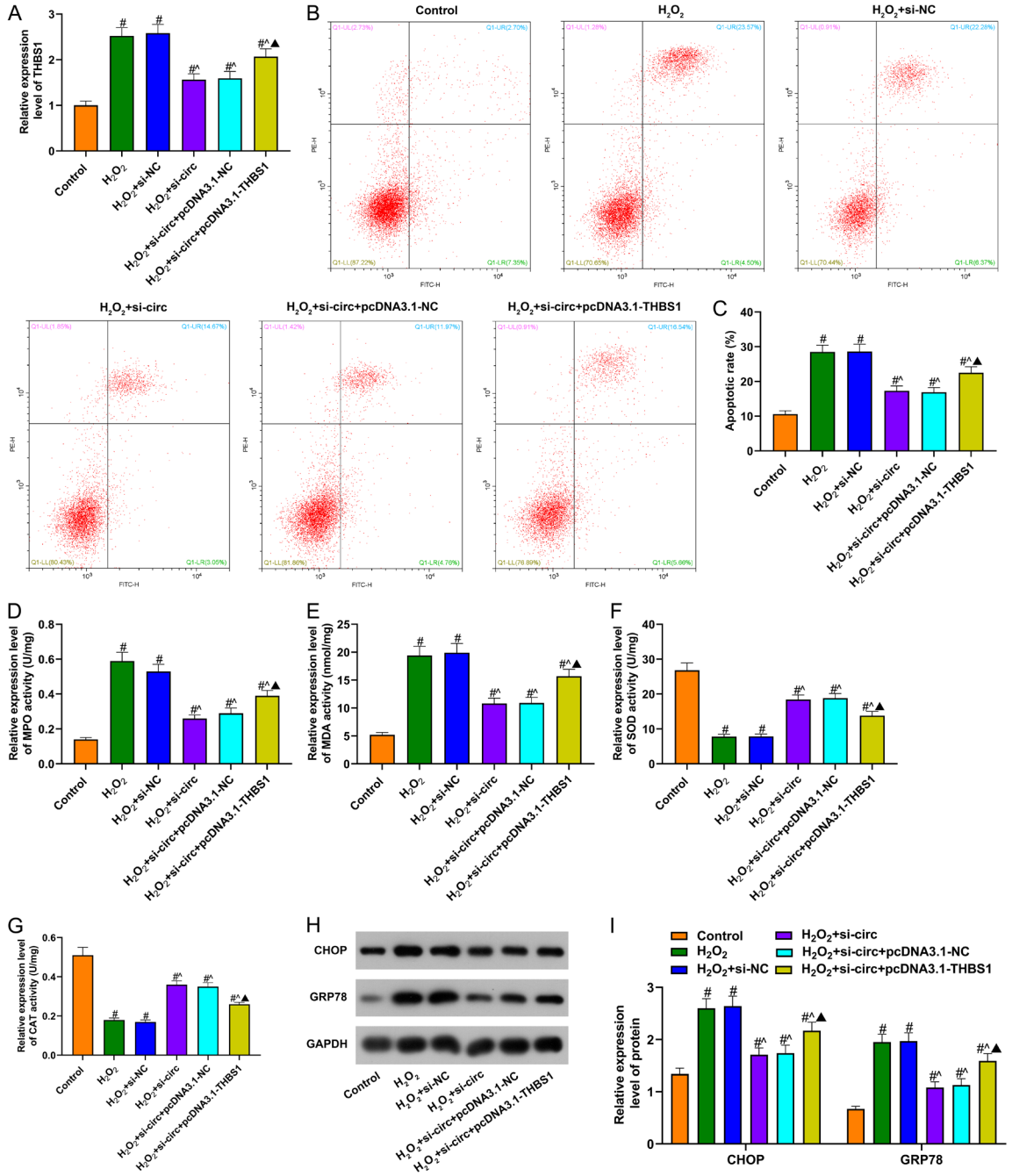

Figure 8. Overexpression of THBS1 partially reversed the neuronal damage reduced by knocking down circ_014260. A: Level of THBS1 measured by qRT-PCR (n=3); B, C: Changes in neuronal apoptosis detected by flow cytometry (n=3); D: Changes in MPO activity measured by Elisa (n=3); E: Changes in MDA activity measured by Elisa (n=3); F: Changes in SOD activity measured by Elisa (n=3); G: Changes in CAT activity measured by Elisa (n=3); H, I: Protein levels of CHOP and GRP78 measured by Western blot (n=3). Compared with control group, #P<0.05; compared with H_2O_2+si-NC group, ^P<0.05; compared with H_2O_2+si-circ+pcDNA3.1-NC group, ▲P<0.05. MPO: myeloperoxidase; MDA: malondialdehyde; SOD: superoxide dismutase; CAT: catalase.

have shown that miR-384-5p plays an important role in cell survival after injuries [21, 22]. Serum miR-384-5p has been reported to be a biomarker of the severity of SCI [23]. Besides, miR-384-5p can increase the survival rate of spinal cord neurons in rats with spinal cord

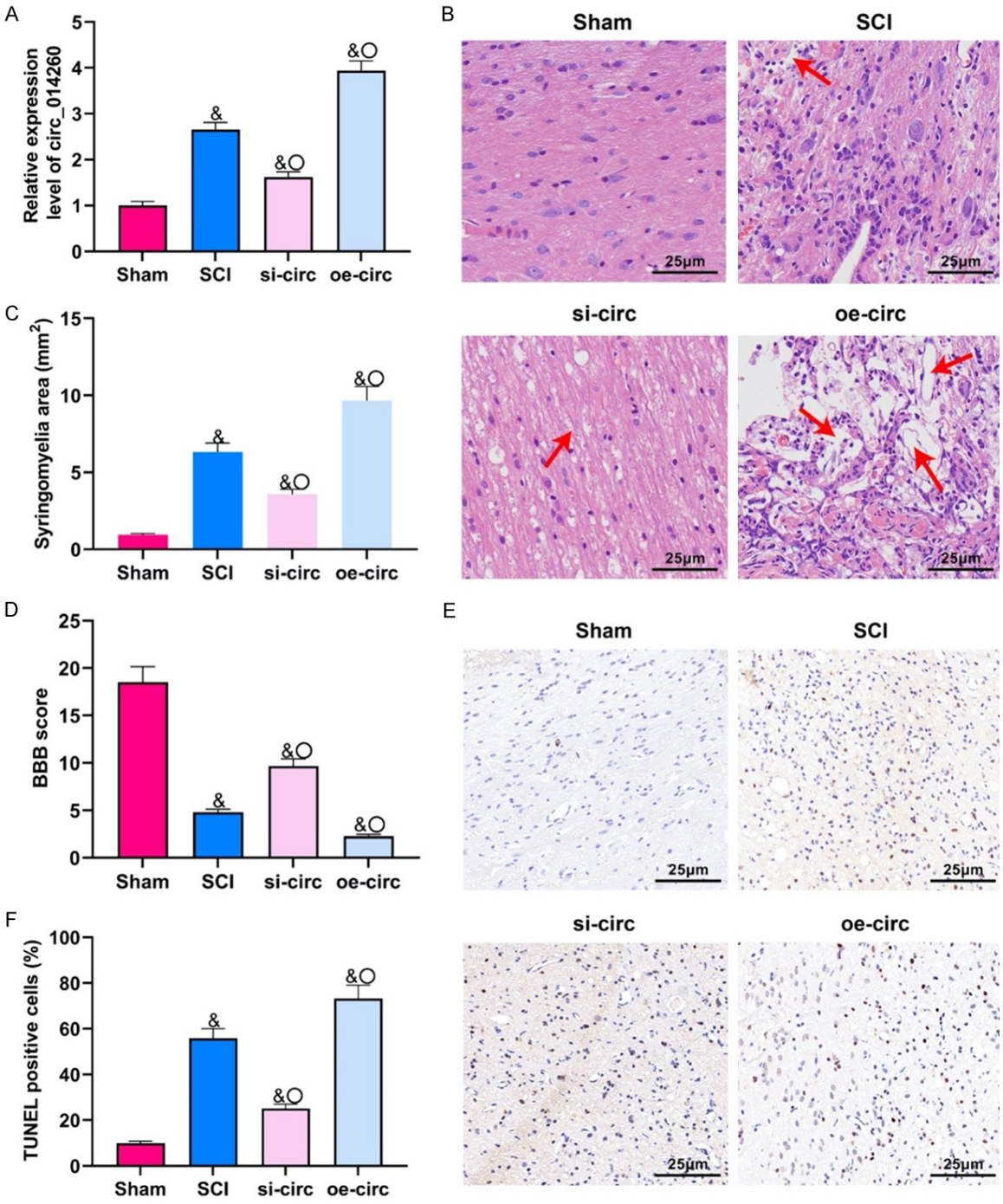

Figure 9. Knockdown of circ_014260 reduced neuronal damage in rats with SCI (n=10). A: Level of circ_014260 measured by qRT-PCR (n=3); B: SCI lesions in rats (HE staining, 400×; n=3); C: Comparison of spinal cavity area in each group (n=3); D: Changes of BBB score in rats with SCI (n=3); E, F: Changes in neuronal apoptosis in spinal cord tissue of rats with SCI (TUNEL staining, 400×; n=3). Compared with sham operation group, $^{\&}P<0.05$; compared with the SCI group, $^{\circ}P<0.05$. SCI: spinal cord injury; BBB: Basso, Beattie & Bresnahan locomotor rating.

compression injury and promote the recovery of motor function [8]. The data of this study showed that miR-384 was down-regulated in both rat model of SCI and the H_2O_2-treated neuronal cells. In the neurons treated with H_2O_2, miR-384 was negatively regulated as the down-

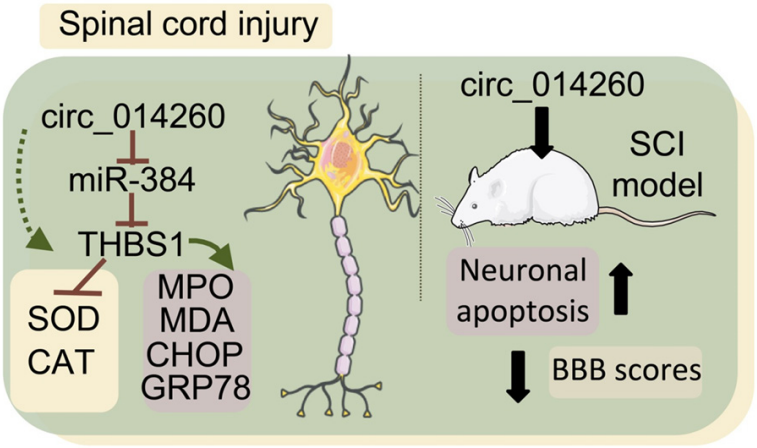

Figure 10. Mechanism of circ_014260/miR-384/THBS1 promoting neuronal apoptosis and endoplasmic reticulum stress and aggravating spinal cord nerve injury in rats.

stream target of circ_014260. Down-regulation of miR-384 partially inhibited neuronal apoptosis, oxidative stress and ERs which were reduced by knocking down circ_014260. It is suggested that circ_014260 can aggravate neuronal damage in rats with SCI by inhibiting miR-384. Enrichment analysis and PPI analysis showed that THBS1 was the downstream target gene of miR-384. Previous study has shown that THBS1 plays an important role in the early stage of neuronal development [24]. Erythropoietin can effectively prevent pathological changes after SCI by reducing the expression of THBS1 [25]. The data of this study showed that expression of THBS1 increased in both rat model of SCI and H_2O_2-treated neuronal cells. *In vitro* experiments showed that circ_014260 up-regulated the expression of THBS1 by inhibiting miR-384, and overexpression of THBS1 partially reversed the alleviated SCI neuronal damage from knocking down circ_014260. It is suggested that circ_014260 can inhibit miR-384 from up-regulating THBS1, which aggravates the SCI neuronal apoptosis, oxidative stress, and ERs.

In summary, our study found that knocking down circ_014260 can up-regulate miR-384 and inhibit THBS1, thereby reducing neuronal apoptosis, oxidative stress, and ERs, as well as restoring motor function in rats with SCI. These findings indicate that circ_014260 may be a promising therapeutic target for SCI. However, this study still has certain limitations. First, the sample size was limited. Second, *in vivo* experiment of the miR-384/THBS1 axis and possible signal pathways regulated by circ_014260 still need to be further studied. Third, it is still challenging to fully understand the mechanism of circ_014260/miR-384/THBS1 in SCI. Therefore, further research is needed to clarify the internal mechanism. The mechanism of this study is shown in **Figure 10**.

Acknowledgements

The study was approved by Natural Science Foundation of Heilongjiang Province of China (JQ2020H003).

Disclosure of conflict of interest

None.

Address correspondence to: Xintao Wang, Department of Orthopedics, The Second Affiliated Hospital of Harbin Medical University, No. 246 Xuefu Road, Harbin 150001, Heilongjiang Province, China. Tel: +86-0451-86662962; E-mail: xintaog6@163.com

References

[1] Yamanaka H, Takata Y, Nakagawa H, Isosaka-Yamanaka T, Yamashita T and Takada M. An enhanced therapeutic effect of repetitive transcranial magnetic stimulation combined with antibody treatment in a primate model of spinal cord injury. PLoS One 2021; 16: e0252023.

[2] Jasim M and Brindha T. Spinal cord segmentation and injury detection using a crow search-rider optimization algorithm. Biomed Tech (Berl) 2021; 66: 293-304.

[3] Wang W, Su Y, Tang S, Li H, Xie W, Chen J, Shen L, Pan X and Ning B. Identification of noncoding RNA expression profiles and regulatory interaction networks following traumatic spinal cord injury by sequence analysis. Aging (Albany NY) 2019; 11: 2352-2368.

[4] Wang WZ, Li J, Liu L, Zhang ZD, Li MX, Li Q, Ma HX, Yang H and Hou XL. Role of circular RNA expression in the pathological progression after spinal cord injury. Neural Regen Res 2021; 16: 2048-2055.

[5] Chen J, Fu B, Bao J, Su R, Zhao H and Liu Z. Novel circular RNA 2960 contributes to secondary damage of spinal cord injury by sponging miRNA-124. J Comp Neurol 2021; 529: 1456-1464.

[6] Wang W, He D, Chen J, Zhang Z, Wang S, Jiang Y and Wei J. Circular RNA plek promotes fibrogenic activation by regulating the miR-135b-5p/TGF-βR1 axis after spinal cord injury. Aging (Albany NY) 2021; 13: 13211-13224.
[7] Peng P, Zhang B, Huang J, Xing C, Liu W, Sun C, Guo W, Yao S, Ruan W, Ning G, Kong X and Feng S. Identification of a circRNA-miRNA-mRNA network to explore the effects of circrnas on pathogenesis and treatment of spinal cord injury. Life Sci 2020; 257: 118039.
[8] Guo XD, He XG, Yang FG, Liu MQ, Wang YD, Zhu DX, Zhang GZ, Ma ZJ and Kang XW. Research progress on the regulatory role of micrornas in spinal cord injury. Regen Med 2021; 16: 465-476.
[9] Zhou Z, Hu B, Lyu Q, Xie T, Wang J and Cai Q. miR-384-5p promotes spinal cord injury recovery in rats through suppressing of autophagy and endoplasmic reticulum stress. Neurosci Lett 2020; 727: 134937.
[10] Wang X, Chen W, Liu W, Wu J, Shao Y and Zhang X. The role of thrombospondin-1 and transforming growth factor-beta after spinal cord injury in the rat. J Clin Neurosci 2009; 16: 818-821.
[11] Li J, Li H, Cai S, Bai S, Cai H and Zhang X. CD157 in bone marrow mesenchymal stem cells mediates mitochondrial production and transfer to improve neuronal apoptosis and functional recovery after spinal cord injury. Stem Cell Res Ther 2021; 12: 289.
[12] Li X, Lou X, Xu S, Du J and Wu J. Hypoxia inducible factor-1 (HIF-1α) reduced inflammation in spinal cord injury via miR-380-3p/NLRP3 by Circ 0001723. Biol Res 2020; 53: 35.
[13] Yuan J, Botchway BOA, Zhang Y, Wang X and Liu X. Role of circular ribonucleic acids in the treatment of traumatic brain and spinal cord injury. Mol Neurobiol 2020; 57: 4296-4304.
[14] Liu Y, Liu J and Liu B. Identification of Circular RNA expression profiles and their implication in spinal cord injury rats at the immediate phase. J Mol Neurosci 2020; 70: 1894-1905.
[15] Zhou ZB, Du D, Chen KZ, Deng LF, Niu YL and Zhu L. Differential expression profiles and functional predication of circular ribonucleic acid in traumatic spinal cord injury of rats. J Neurotrauma 2019; 36: 2287-2297.
[16] You X, Vlatkovic I, Babic A, Will T, Epstein I, Tushev G, Akbalik G, Wang M, Glock C, Quedenau C, Wang X, Hou J, Liu H, Sun W, Sambandan S, Chen T, Schuman EM and Chen W. Neural circular RNAs are derived from synaptic genes and regulated by development and plasticity. Nat Neurosci 2015; 18: 603-610.
[17] Shahid M, Subhan F, Islam NU, Ahmad N, Farooq U, Abbas S, Akbar S, Ullah I, Raziq N and Din ZU. The antioxidant N-(2-mercaptopropionyl)-glycine (tiopronin) attenuates expression of neuropathic allodynia and hyperalgesia. Naunyn Schmiedebergs Arch Pharmacol 2021; 394: 603-617.
[18] Jiang W, Li M, He F, Yao W, Bian Z, Wang X and Zhu L. Protective effects of asiatic acid against spinal cord injury-induced acute lung injury in rats. Inflammation 2016; 39: 1853-1861.
[19] Zhao L, Zhai M, Yang X, Guo H, Cao Y, Wang D, Li P and Liu C. Dexmedetomidine attenuates neuronal injury after spinal cord ischaemia-reperfusion injury by targeting the CNPY2-endoplasmic reticulum stress signalling. J Cell Mol Med 2019; 23: 8173-8183.
[20] Zhu Y, Zhang L, Fu R, Gao L, Feng G, Du C, Wang Z and Yan X. The change tendency of endoplasmic reticulum stress associated proteins in rats with spinal cord injury. Am J Transl Res 2019; 11: 1938-1947.
[21] Bao Y, Lin C, Ren J and Liu J. MicroRNA-384-5p regulates ischemia-induced cardioprotection by targeting phosphatidylinositol-4,5-bisphosphate 3-kinase, catalytic subunit delta (PI3K p110δ). Apoptosis 2013; 18: 260-270.
[22] Jiang M, Yun Q, Shi F, Niu G, Gao Y, Xie S and Yu S. Downregulation of miR-384-5p attenuates rotenone-induced neurotoxicity in dopaminergic SH-SY5Y cells through inhibiting endoplasmic reticulum stress. Am J Physiol Cell Physiol 2016; 310: C755-763.
[23] Hachisuka S, Kamei N, Ujigo S, Miyaki S, Yasunaga Y and Ochi M. Circulating microrna as biomarkers for evaluating the severity of acute spinal cord injury. Spinal Cord 2014; 52: 596-600.
[24] Bray ER, Yungher BJ, Levay K, Ribeiro M, Dvoryanchikov G, Ayupe AC, Thakor K, Marks V, Randolph M, Danzi MC, Schmidt TM, Chaudhari N, Lemmon VP, Hattar S and Park KK. Thrombospondin-1 mediates axon regeneration in retinal ganglion cells. Neuron 2019; 103: 642-657, e647.
[25] Fang XQ, Fang M, Fan SW and Gu CL. Protection of erythropoietin on experimental spinal cord injury by reducing the expression of thrombospondin-1 and transforming growth factor-beta. Chin Med J (Engl) 2009; 122: 1631-1635.